16,09

Effect of Stoichiometric Defects on the Raman Spectrum and Polarization Anisotropy in a Two-Dimensional CrSBr Magnetic Semiconductor

© D.L. Gusenkov[1,2], E.O. Chiglintsev[3,4], A.I. Chernov[3,4], V.V. Savin[1], R.B. Morgunov[1,2,4,5,¶]

[1] Federal Research Center of Problems of Chemical Physics and Medicinal Chemistry RAS, Chernogolovka, Russia
[2] Sechenov First Moscow State Medical University, Ministry of Health of the Russian Federation, Moscow, Russia
[3] Center of Photonics and 2D Materials, Moscow Institute of Physics and Technology, Dolgoprudny, Russia
[4] Russian Quantum Center, „Skolkovo", Innovation Center, Moscow, Russia
[5] Immanuel Kant Baltic Federal University, Kaliningrad, Russia
[¶] E-mail: spintronics2022@yandex.ru

Received October 26, 2025
Revised January 19, 2026
Accepted January 27, 2026

The two-dimensional CrSBr magnetic semiconductor is of considerable interest for spintronics. However, its functional properties critically depend on the stoichiometry and the quality of the crystal lattice. In this paper, we present studies of the optical properties of CrSBr samples characterized by different stoichiometry, bromine deficiency, and the presence of the Cr_2S_3 impurity phase. Raman polarization spectroscopy revealed that such defects lead to a decrease in the intensity of the main vibrational modes, their broadening and frequency shift. The results obtained demonstrate that RAMAN spectroscopy is an effective, non-destructive method for rapid assessment of the stoichiometry and quality of CrSBr crystals, which is of paramount importance for reproducibility of their magnetic and optical properties.

Keywords: two-dimensional semiconductors, stoichiometry, Raman spectroscopy, X-ray fluorescence analysis.

DOI: 10.61011/PSS.2026.02.63392.300-25

1. Introduction

Two-dimensional (2D) materials featuring an atomic thickness and a weak van der Waals bonding between the layers have opened up new horizons in condensed matter physics and nanoelectronics [1–3]. Among them, anisotropic magnetic semiconductors are of particular interest, combining semiconductor behavior with magnetic ordering, which makes them promising for spintronics and quantum technologies [4,5]. A key requirement for the practical application of such materials is the stability of their properties, which directly depends on the quality of the crystal lattice, stoichiometry, and degree of texturing of polycrystals [6–8]. One of the most effective non-destructive methods for probing these parameters is polarization-resolved Raman spectroscopy (RS). This method allows not only to identify the phase composition and the number of layers, but also to determine the crystallographic orientation, local stresses, degree of order, and anisotropic electron-phonon interaction in low-symmetry crystals [7,8]. In orthorhombic 2D materials (e.g., black phosphorus, ReS_2, CrSBr), the angular dependence of the intensity of modes active in RS spectra is used to determine the crystal symmetry [7,8]. Recent studies have shown that the position of peaks in frequency can also carry information about resonant electronic transitions and local anisotropy [9].

Among the Van der Waals semiconductors CrSBr holds a special place — its itself a layered compound with an orthorhombic structure ($Pmmn$, point group D_{2h}) exhibiting A-type of antiferromagnetism ($T_N \approx 132\,K$) and quasi-one-dimensional nature of the electronic structure [5,10]. CrSBr exhibits strong optical and electrotransport anisotropy, as well as spin-phonon interactions sensitive to structural defects [10–12]. RS spectra of CrSBr are characterized by the three major symmetry modes A_g: A_g^1 ($\sim 114\,cm^{-1}$), A_g^2 ($\sim 244\,cm^{-1}$) and A_g^3 ($\sim 344\,cm^{-1}$) indicating the vibrations of Br, Cr and S atoms [10,12] in the layers plane and perpendicular to the layers.

A critical feature of CrSBr is its sensitivity to stoichiometric disturbances: even a small bromine deficiency leads to the appearance of a characteristic defective mode D1 ($\sim 110\,cm^{-1}$), line broadening, and changes in magnetic properties [10,12]. Moreover, recent studies have shown that the mode A_g^2 exhibits resonant polarization switching depending on the excitation energy: at 2.33 eV, it is polarized along the magnetically intermediate axis a, and at lower energies — along the light magnetic axis b [13]. This phenomenon is explained by the anisotropy of RS tensor and the resonant electron-phonon interaction associated with

a quasi-one-dimensional electronic structure [10,13]. Such effects make RS spectroscopy not only a structural, but also an electron-sensitive method.

Most studies of RS spectra were performed on exfoliated flakes with a thickness from a monolayer to several atomic layers with a controlled crystal-lattice orientation. At the same time, bulky polycrystalline samples used in crystal cultivation are characterized by a random grain orientation, local stresses, and an inhomogeneous distribution of defects. In such systems, the signal represents an averaged contribution from multiple disoriented crystallites, which leads to an inhomogeneous broadening of the lines, weak anisotropy, and, possibly, to suppression of the dependence of lines positions on the orientation of the light polarization plane relative to the crystalline planes [7,8].

This study is aimed at analyzing the effect of stoichiometry and polycrystalline texture of flakes and bulk polycrystals of CrSBr on the anisotropy of the polarization-resolved RS spectra.

2. Methodology and samples

Two types of commercial CrSBr crystals were used for the experiments. Sample 1 was purchased from „2D Semiconductors“, and sample 2 was grown at „HQ graphene“. The magnetic and mechanical properties of these samples have been described by us in previous studies [14,15]. The thickness of the samples was $\sim 0.01-0.5$ mm and significantly exceeded the thickness of the monomolecular layer, which made it possible to ignore the features associated with nanoscale samples.

The samples' chemical composition was determined using energy dispersive X-ray spectroscopy (EDX) on a scanning electron microscope Zeiss LEO SUPRA 25. This technique is based on the excitation of intra-atomic transitions by X-ray radiation, followed by the emission of photons, the frequency of which identifies the atoms in the sample. Its usage was dictated by the need of stoichiometry control.

RS spectroscopy makes it possible to determine the vibrational frequencies of a lattice, and RS spectra depend not only on the chemical composition, but also on the crystal structure of the material itself. The wavelengths longer than in X-ray radiation used in RS spectroscopy do not excite internal electronic transitions in atoms and therefore cannot be used to identify chemical elements. Nevertheless, the RS spectroscopy method makes it possible to distinguish the phases present in the sample by the characteristic frequencies of atomic vibrations.

The RS spectra were registered at room temperature on a confocal spectrometer Confotec NR500. A solid-state laser with a wavelength of 532 nm (photon energy 2.33 eV) and an output power of 16 mW per sample was used as the excitation source. The laser radiation was focused and RS signal was registered using the lens 40×. A diffraction grating with a density of 1800 lines/mm was installed in the spectrometer, providing a spectral resolution of $\sim 0.9\,\mathrm{cm}^{-1}$.

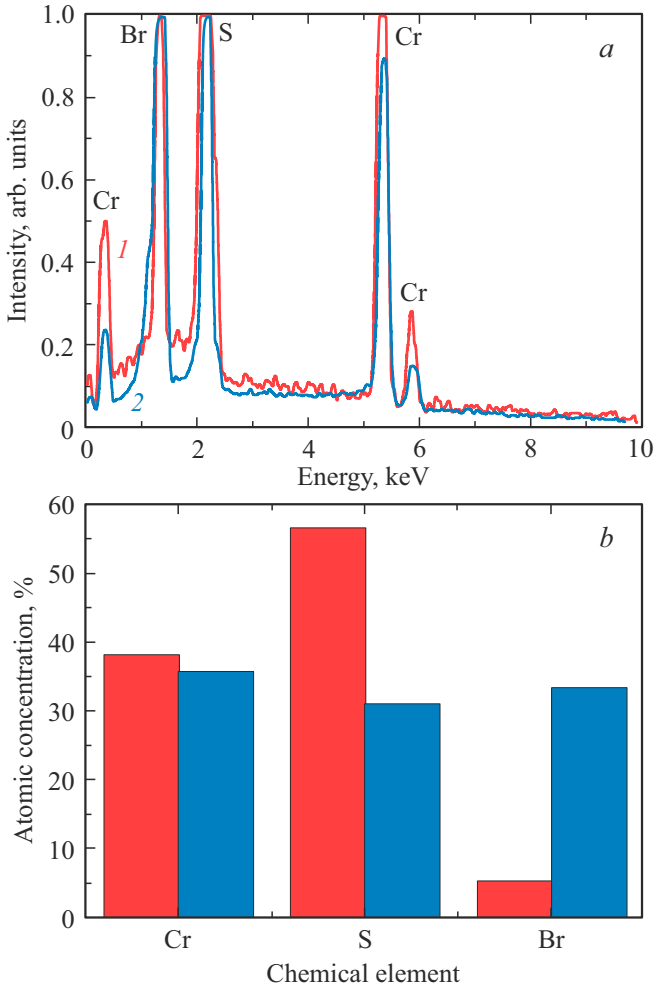

Figure 1. *a* — EDX spectra of sample 1 (red line, *1*) and sample 2 (blue line, *2*). *b* — chemical composition of sample 1 (red color) and sample 2 (blue color).

The lateral spatial resolution of the system, determined by the size of the diffraction-limited focal spot, was ~ 500 nm.

To measure the angular dependence of the spectrum, the sample was rotated in the plane *ab* relative to a stationary laser beam with a step of 10° in the range from 0° to 350°. Polarization of the exciting and scattered light was parallel to the axis *a* at reference point. The device was calibrated using a silicon sample with its peak in RS spectrum at $520.5\,\mathrm{cm}^{-1}$.

3. Experimental results and discussion

3.1. Chemical composition and atomic structure

Figure 1, *a* illustrates EDX spectra for samples 1 and 2 respectively. Both of the samples have similar spectra, yet, the ratio of peak intensities in these spectra indicates a difference in their stoichiometry. Results of the quantitative analysis of chemical element concentrations in both samples are shown in Figure 1, *b*.

RS spectroscopy data in samples 1 and 2 and literature data for the lines A_g^1, A_g^2, A_g^3

		Sample 1	Sample 2	CrSBr from [10]
A_g^1	Peak position, cm^{-1}	115.3	114.5	114
	Peak width, cm^{-1}	5.47	6.75	–
A_g^2	Peak position, cm^{-1}	246.9	244.3	244
	Peak width, cm^{-1}	5.27	3.65	–
A_g^3	Peak position, cm^{-1}	347.9	343.9	344
	Peak width, cm^{-1}	7.24	9.08	–

According to the structural formula, the samples shall have equal concentrations of all atoms. However, sample 1 has a considerable stoichiometry deviation due to the lack of bromine. Chemical composition of sample 2 corresponds to that specified by the manufacturer.

3.2. RS spectrum and identification of modes

According to the calculated data, within the density functional theory (DFT), the RS spectrum of the stoichiometric CrSBr with polarization of light along the axis b demonstrates three main modes: A_g^1 ($\sim 114\,cm^{-1}$), A_g^2 ($\sim 244\,cm^{-1}$) and A_g^3 ($\sim 344\,cm^{-1}$) [10]. The mode A_g^1 is associated with out-of-plane vibrations of bromine atoms, A_g^2 — with vibrations of Cr, S and Br, and the mode A_g^3 — mainly with vibrations of Cr and S in the plane. Vibrations of atoms in the lattice, as well as specific contribution of atoms to the formation of modes, as illustrated by the arrows of appropriate lengths, are shown in Figure 2. Figure 3 shows RS-spectra of both samples.

When flake is mechanically split off from sample 1, two types of micro-samples are obtained: faceted plates (Figure 4, a) and shapeless flakes (Figure 4, b). Their RS spectra differ significantly. RS spectrum of light scattering for a crystal in the form of shapeless flakes is shown in Figure 3, a. A detailed study of this type of crystals is presented in our previous article [14]. It is worth noting that for shapeless flakes, it was not possible to obtain dependencies on the direction of light polarization. This is probably due to a large proportion of substitution of CrSBr phase by Cr_2S_3 phase and disorientation of the grains of the resulting new phase, which makes the spectra isotropic.

In the spectrum of sample 1, which retained a rectangular crystallographic cut, there is a significant redistribution of the intensity of all three modes and a shift in peak positions (Figure 3, b) compared with the perfect chemical composition of sample 2 (Figure 3, c). In addition, the identified peaks show a decrease in their width by half the height (FWHM), with the exception of the peak A_g^2.

The following table contains quantitative indicators of the lines of RS spectrum for both types of samples and literature data. The most convincing evidence of bromine depletion is the appearance of an additional peak D1 (see Figure 3, d) at $\sim 110\,cm^{-1}$ and located by $\sim 5-10\,cm^{-1}$ below the principal mode A_g^1. This peak fully corresponds to D1 mode associated with defects previously identified as bromine vacancies on the surface, which occur, in particular, during hydrolysis [10]. The presence of peak of D1 in sample 1 is a direct evidence of bromine deficiency, which was also detected by EDX method. At the same time, the spectrum of a chemically perfect sample 2 does not contain such a mode (see Figure 3, c).

3.3. RS spectrum versus light polarization angle

Figure 5 shows RS spectra at different angles between the plane of polarization of light and plane ab. Measurements were made with a step 10°.

The angular dependences of the intensities of modes A_g^1, A_g^2 and A_g^3, shown in Figure 6, $a-c$, demonstrate a sinusoidal dependence with a period of 180° for both studied samples. This behavior is fully consistent with the orthorhombic crystal symmetry of CrSBr (space group $Pmmn$, group of dots D_{2h}) and theoretical predictions for symmetry modes A_g^i [7,8]. For symmetry modes A_g^i in the orthorhombic CrSBr crystal (group D_{2h}), the RS tensor determining the intensity of spectral lines is a diagonal [13]:

$$R_(A_g) = \begin{pmatrix} R_{xx} & 0 & 0 \\ 0 & R_{yy} & 0 \\ 0 & 0 & R_{zz} \end{pmatrix},$$

where $x \equiv a$, $y \equiv b$, $z \equiv c$ — crystallographic axes. When light is polarized in plane ac, the intensity dependence of the peaks obtained under resonant conditions is described by the formula:

$$I(\alpha) = (R_{xx}\cos^2\alpha + R_{yy}\sin^2\alpha).$$

As a result the intensity maxima for the modes A_g^1 and A_g^3 were observed at angles of 0 and 180° (polarization along the axis a), since the mode A_g^2 reaches its maximum at 90° and 270° (polarization along the axis b). The normalized experimental curves for the stoichiometric sample 2 are consistent with the data obtained in the literature [13] for the 62 nm thick CrSBr sample at an excitation energy of 2.33eV,

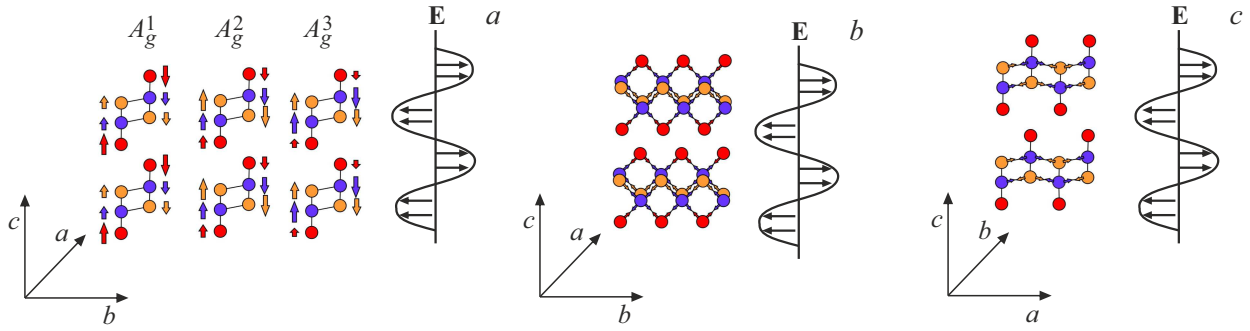

Figure 2. Diagram of atoms vibration in the modes A_g^1, A_g^2. (*a*) Arrows indicate specific contribution of an atom vibration per mode. (*b*) Lattice vibration along crystallographic axis *a* under vibrations of electric field vector *E* in the plane *bc*. (*c*) Lattice vibration along crystallographic axis *b* under vibrations of electric field vector *E* in the plane *ac*. Blue symbols — chromium atoms, orange symbols — sulfur atoms, red symbols — bromine atoms.

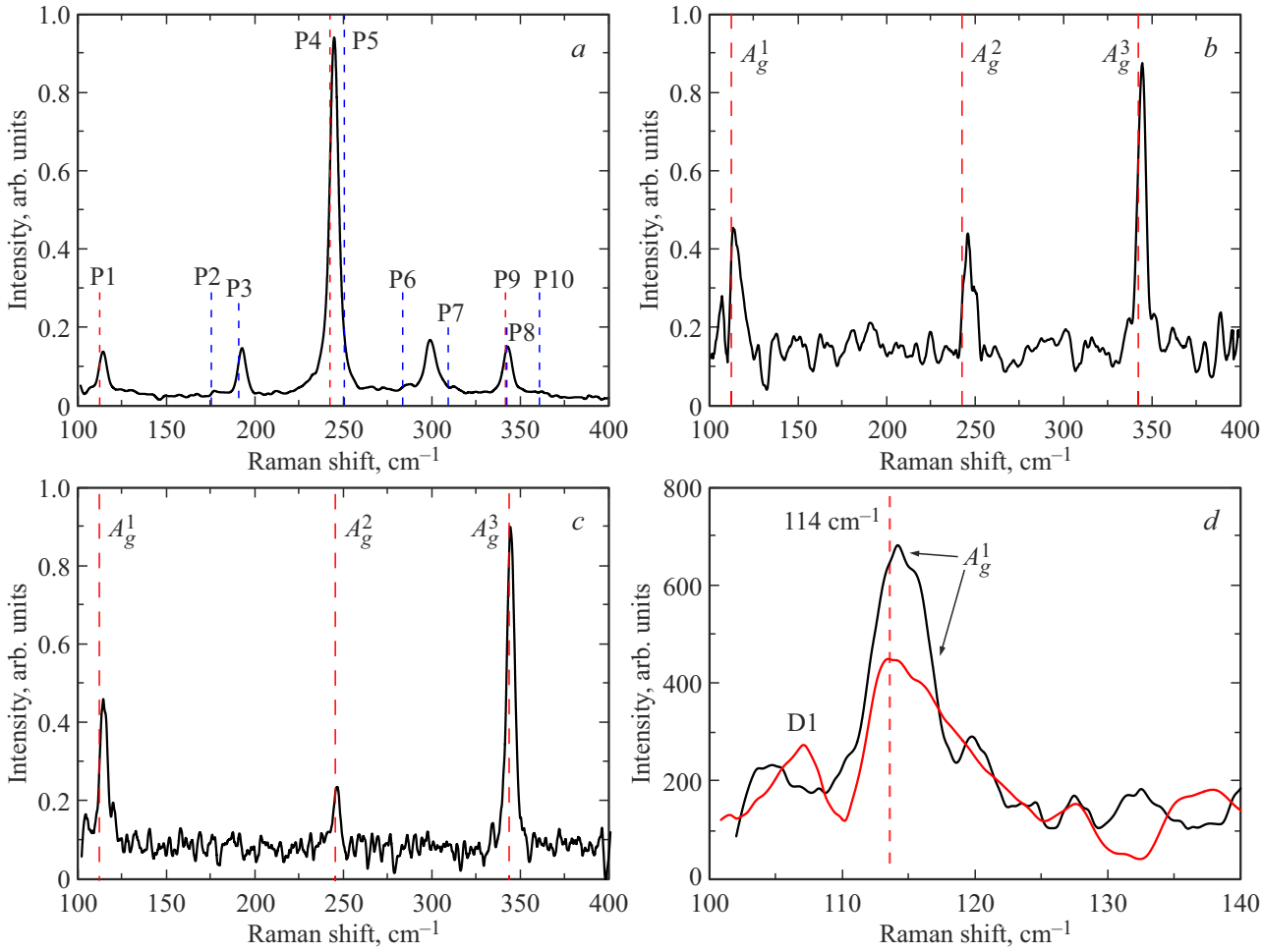

Figure 3. *a* — RS spectrum of sample 1 in shapeless flakes when the plane of light polarization is oriented in the plane *bc*. The red dotted lines — are the peak positions for CrSBr in the literature [16], the blue dotted lines — are the peak positions Cr_2S_3, taken from the literature [12]. *b* — RS spectrum of a faceted sample fragment 1 when the plane of light polarization is oriented in the plane *bc*. *c* — RS spectrum of sample 2 when the plane of light polarization is oriented in the plane *bc*. *d* — comparison of RS spectra of samples 1 and 2 near A_g^1 mode. Black line — RS spectrum of sample 2. Red line — RS spectrum of sample 1.

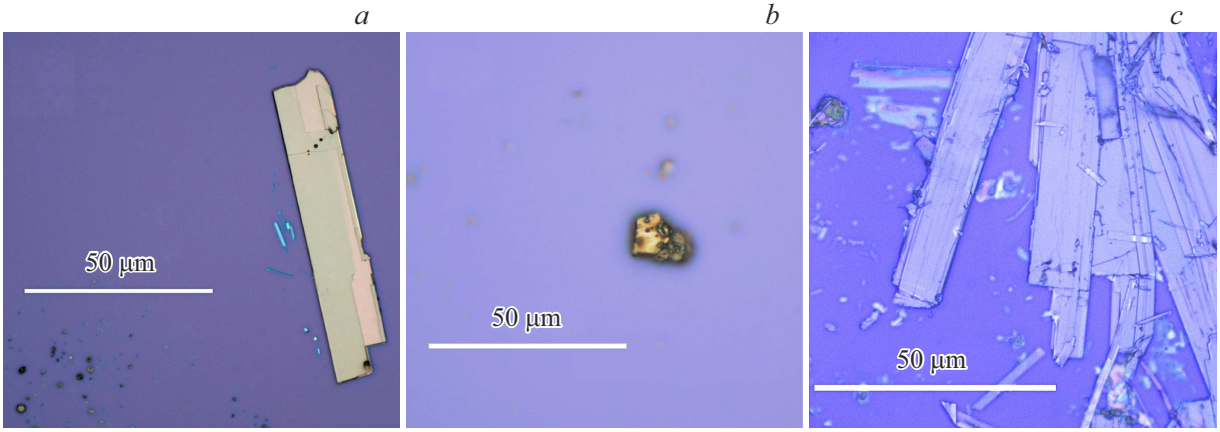

Figure 4. Micrographs of faceted crystals (*a*) and shapeless flakes (*b*) of sample 1, and faceted crystals of sample 2 (*c*).

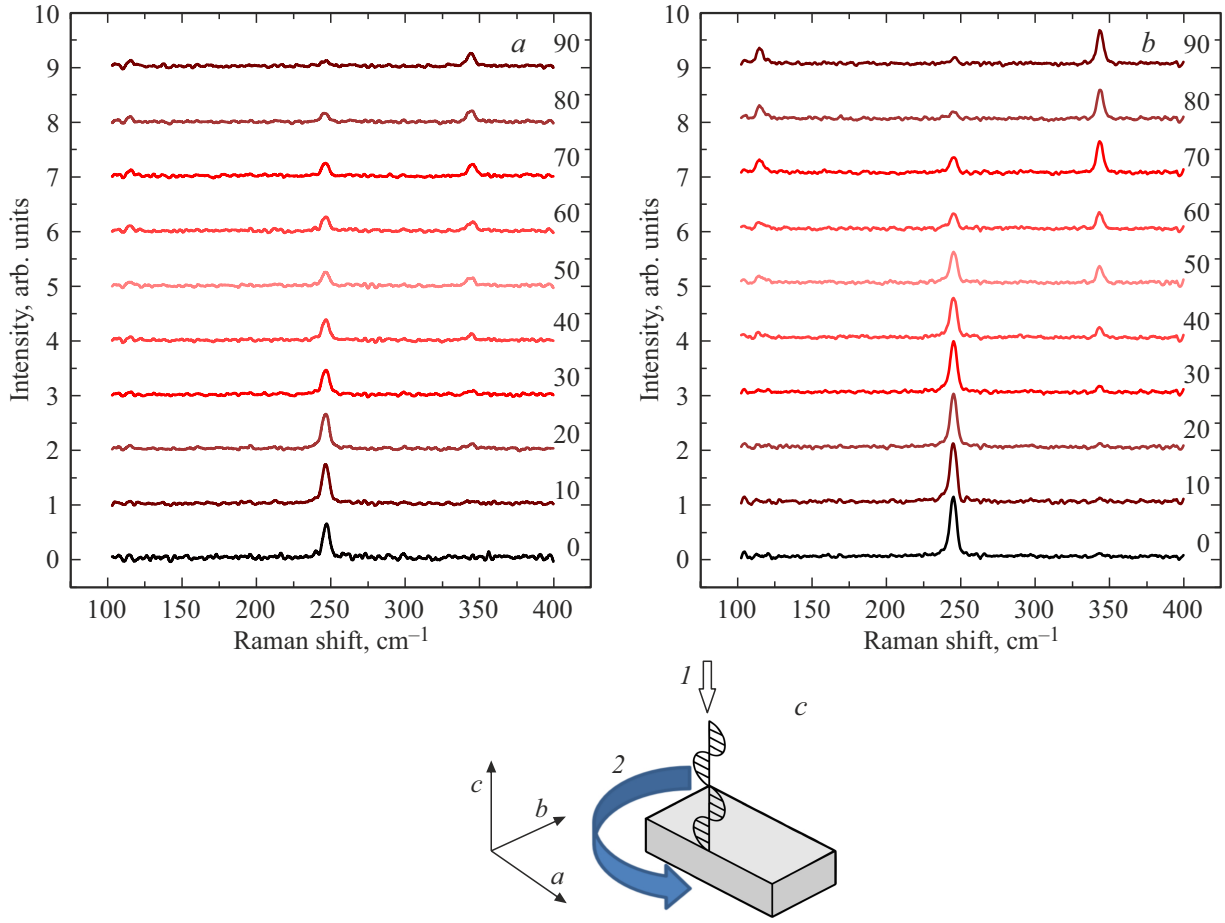

Figure 5. RS spectra of sample 1 (*a*) and sample 2 (*b*) at different angles between the polarization light plane and plane *ac* (*c*), angle 0° corresponds to a situation when the light polarization plane lies in the plane *ca* (*1*), and angle 90° — in the plane *bc*. The sample was rotated around the axis *c* (*2*).

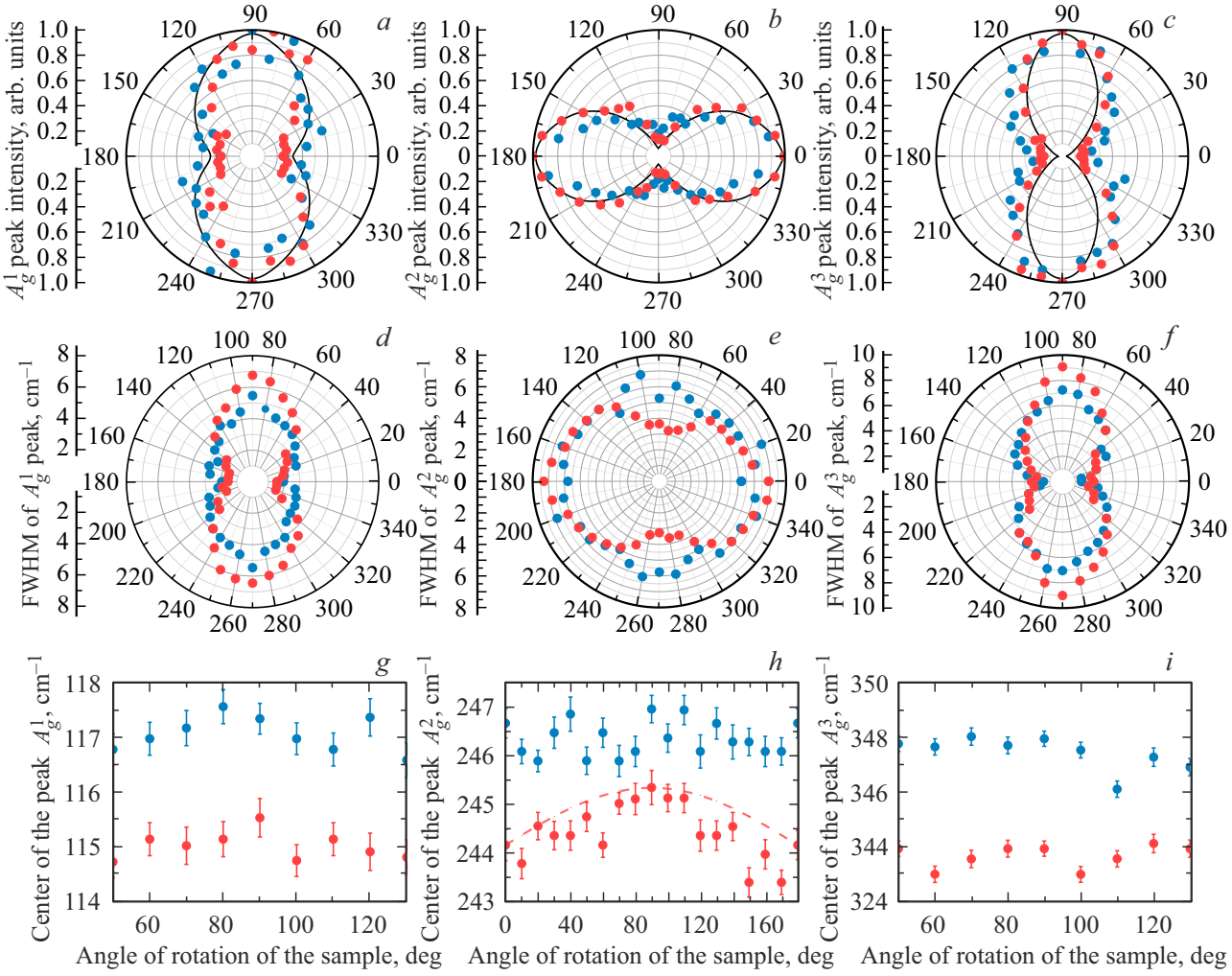

Figure 6. Normalized intensities of peaks A_g^1 (*a*), A_g^2 (*b*) and A_g^3 (*c*) versus the angle between the polarization plane and the lattice plane *ac*: dot glow — data for sample 1, red dots — data for sample 2, black line — data for CrSBr sample with a thickness of 62 nm [13]. FWHM of peaks A_g^1 (*d*), A_g^2 (*e*) and A_g^3 (*f*) versus the sample rotation angle α. The positions of the centers of peaks A_g^1 (*g*), A_g^2 (*h*) and A_g^3 (*i*) versus the sample rotation angle: blue dots — data for sample 1, red dots — data for sample 2, red dotted line — approximation of the position of peaks of sample 2 by a sinusoidal function.

which confirms the correctness of our measurements and the high quality of the crystal.

It should be emphasized that the crystals Cr_2S_3 have a rhombohedral lattice with the spatial group $R\bar{3}$, which corresponds to 120°-periodicity of the modes [17]. Therefore, possible deviations from the ideal 180°-symmetry observed in the angular dependences in sample 1 may be related to the presence of this phase. The phase Cr_2S_3 which has a different symmetry, can contribute to a signal that does not obey the 180°periodicity, which leads to disturbances in the form of polar diagrams.

The analyzed FWHM peaks in Figure 6, *d*–*f* show some difference between the samples 1 and 2: in the sample 1 a significant broadening of modes A_g^1 and A_g^3 is observed at angles of 0 and 180°. There are also differences in the symmetry of the intensity and FWHM of A_g^2 line in sample 1. The intensity of the line is maximal at an angle $\alpha = 0$ between the plane of polarization and the lattice plane *ac*, and the width of this line and the position of its center are practically isotropic with accuracy to a measurement error. This means that sample 1 contains a phase in which atomic vibrations are more isotropic.

The key difference between the samples is manifested in the angular pattern of the peak A_g^2 position. In the stoichiometric sample 2, there is an angular dependence of its resonant frequency with the amplitude $\sim 1.5\,\text{cm}^{-1}$ (Figure 6, *e*), while in the defective sample 1 this dependence is practically absent. This observation cannot be explained within the classical Raman scattering theory, where the peak position is determined only by the phonon dispersion. A similar effect was previously observed under resonant conditions, when the energy of the exciting photon is close to the interband transition in the material (~ 2.0–2.2 eV for CrSBr [10,13]). In [13], it was shown that it is A_g^2

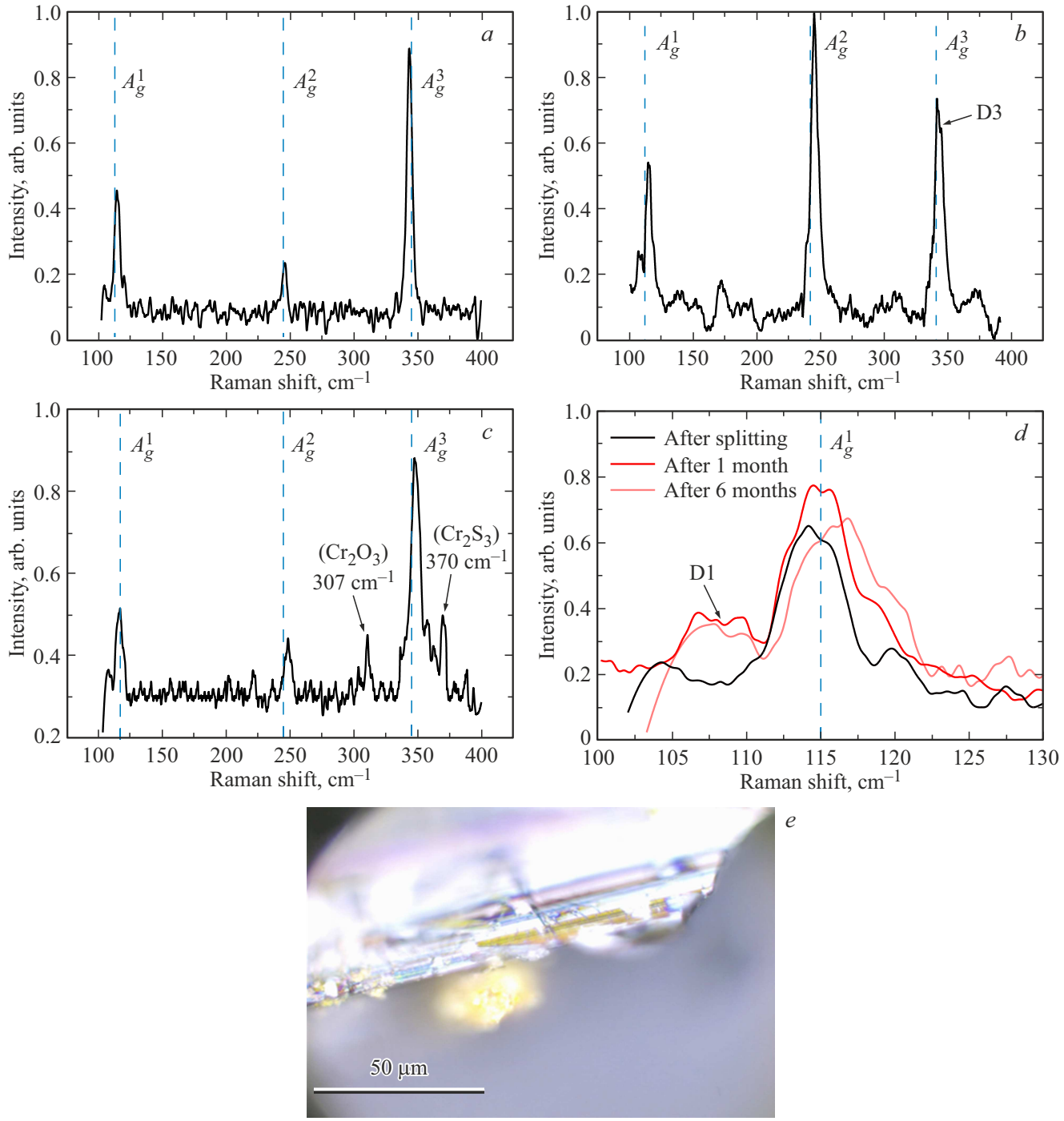

Figure 7. RS spectrum of sample 2 right after mechanical splitting (a), in a month after splitting (b) and in 6 months after splitting (c). d — spectra A_g^1 and D1, registered in different time passed after exfoliation. The blue dotted lines show the positions of CrSBr peaks. e — micrography of the test sample 6 months after the experiment.

mode in CrSBr that exhibits resonant polarization switching at a threshold laser power and is sensitive to the anisotropy of the electronic structure. At an energy of 2.33 eV, its response is determined by the complex elements of RS tensor and the phase shift between the components R_{xx} and R_{yy}. As a result, the effective phonon frequency becomes dependent on the angle between the light polarization and the crystallographic axes. The observation of the angular dependence of the resonant frequency confirms the presence of this effect in high-quality crystals 2. The absence of such a dependence in the defective sample 1 is explained by two factors. First, bromine deficiency and the presence of an impurity phase Cr_2S_3 destroy the local crystal symmetry and suppress the coherent electronic state necessary for

the resonance enhancement. Secondly, because of the polycrystalline structure of the sample the signal may be averaged over a set of disoriented grains. Even if individual domains exhibit an anisotropic response, their contribution to the total spectrum is mutually compensated. Analysis of the shape of A_g^2 line showed that it is closer to the Gaussian shape rather than to the Lorentz shape, which indicates an inhomogeneous broadening associated with variations in RS spectra in different parts of the sample.

Thus, the presence or absence of an angular dependence of the peak frequency A_g^2 serves as a direct and highly sensitive criterion of crystal quality. Unlike the peak intensity or peak width analysis, this parameter provides information not only about the structural, but also about the electronic properties of the material, including quasi-one-dimension of its electrical properties [10,13].

3.4. Degradation in the air

After the sample 2 was measured again one month after mechanical splitting, as shown in Figure 7, the appearance of a weak but reproducible peak D1 was discovered. This an evidence of the fact that even stoichiometrically regular CrSBr crystals are susceptible to degradation in the air, which is accompanied by the formation of bromine vacancies. Apart from the sublimation of bromine, oxidation also affects not only the surface layers, but also leads to formation of interlayer defects affecting chromium and sulfur atoms, which changes the peak D3.

6 months after splitting, visible brown-yellow inclusions were observed on the crystal surface (Figure 7, *d*). RS spectrum on the surface of the sample shown in Figure 7, *c*, demonstrates the appearance of the new phases. Two additional peaks at $\sim 307\,\mathrm{cm}^{-1}$ and $\sim 370\,\mathrm{cm}^{-1}$ are observed. The peak centered at $307\,\mathrm{cm}^{-1}$, characteristic of chromium oxide Cr_2O_3 [18], indicates that the sample's surface layers become oxidative in the open air. The peak at $370\,\mathrm{cm}^{-1}$ combined with the broadening of lines at $\sim 244\,\mathrm{cm}^{-1}$ and $\sim 344\,\mathrm{cm}^{-1}$ can be associated with the formation of the bromine-deficient phase Cr_2S_3 [17].

4. Conclusion

In this study, the effect of stoichiometric defects on the optical properties of CrSBr crystals was investigated using EDX method and polarization-resolved RS spectroscopy. It was found that bromine deficiency leads to a lower intensity and broadening of the base peaks A_g^i, and surface oxidation causes the appearance of a characteristic defect mode D1. The dependence of the parameters of RS spectra on the angle between the plane of light polarization and the crystallographic axes confirmed the orthorhombic symmetry of stoichiometric and non-stoichiometric samples. The heterogeneous broadening of the peaks in the nonstoichiometric sample indicates variations in RS conditions in different parts of the sample.

RS spectroscopy, especially in combination with the study of the spectrum angular dependence, is an express method of quality control of CrSBr crystals. The presence/absence of mode D1, the sinusoidal dependence of the intensity of modes A_g^i and the stability of their position in frequency can serve as reliable criteria for sampling before use in the ready-made devices or other studies. This is critical for reproducibility of the results in studies on spin-phonon interaction and magnetic phase transitions in this promising material.

Funding

The study was carried out within the grant of the Russian Science Foundation No. 25-72-31032, https://rscf.ru/project/25-72-31032/.

Conflict of interest

The authors declare that they have no conflict of interest.

References

[1] K.S. Novoselov, A.K. Geim, S.V. Morozov, D. Jiang, Y. Zhang, S.V. Dubonos, I.V. Grigorieva, A.A. Firsov. Science **306**, 666 (2004).
[2] A. Liu, X. Zhang, Z. Liu, X. Xuan, B.I. Yakobson, M.C. Hersam, W. Guo. Nano-Micro Lett. **16**, 119 (2024).
[3] B. Huang, G. Clark, E. Navarro-Moratalla, D.R. Klein, R. Cheng, K.L. Seyler, D. Zhong, E. Schmidgall, M.A. McGuire, D.H. Cobden, W. Yao, D. Xiao, P. Jarillo-Herrero, X. Xu. Nature **546**, 270 (2017).
[4] C. Gong, L. Li, Z. Li, H. Ji, A. Stern, Y. Xia, T. Cao, W. Bao, C. Wang, Y. Wang, Z.Q. Qiu, R.J. Cava, S.G. Louie, J. Xia, X. Zhang. Nature **546**, 265 (2017).
[5] E.J. Telford, A.H. Dismukes, K. Lee, R.A. Wiscons, J. Wang, X. Xu, C. Nuckolls, C.R. Dean, X. Roy, X. Zhu. Adv. Mater. **32**, 2003240 (2020).
[6] K. Lee, A.H. Dismukes, E.J. Telford, R.A. Wiscons, J. Wang, X. Xu, C. Nuckolls, C.R. Dean, X. Roy, X. Zhu. Nano Lett. **21**, 3511 (2021).
[7] M.A. Pimenta, G.C. Resende, H.B. Ribeiro, B.R. Carvalho. Phys. Chem. Chem. Phys. **23**, 27103 (2021).
[8] H.B. Ribeiro, M.A. Pimenta, C.J.S. de Matos, R.L. Moreira, A.S. Rodin, J.D. Zapata, E.A.T. de Souza, A.H.C. Neto. ACS Nano **9**, 4270 (2015).
[9] N. Mao, X. Wang, Y. Lin, B.G. Sumpter, Q. Ji, T. Palacios, S. Huang, V. Meunier, M.S. Dresselhaus, W.A. Tisdale, L. Liang, X. Ling, J. Kong. J. Am. Chem. Soc. **141**, 18994 (2019).
[10] K. Torres, A. Kuc, L. Maschio, T. Pham, K. Reidy, L. Dekanovsky, Z. Sofer, F.M. Ross, J. Klein. Adv. Funct. Mater. **33**, 2211366 (2023).
[11] J. Klein, Z. Song, B. Pingault, F. Dirnberger, H. Chi, J.B. Curtis, R. Dana, R. Bushati, J. Quan, L. Dekanovsky, Z. Sofer, F.M. Ross. Nano Lett. **13**, 5092 (2022).
[12] A. Gayen, G.H. An, I.N. Rahman, M. Choi, Q. Mustaghfiroh, P.V. Gaikwad, E.S.H. Kang, K.-H. Kim, C. Liu, K. Kim, J. Bang, H.S. Lee, D.-H. Kim. Nanoscale **16**, 17452 (2024).

[13] P. Mondal, D.I. Markina, L. Hopf, L. Krelle, S. Shradha, J. Klein, M.M. Glazov, I. Gerber, K. Hagmann, R.V. Klitzing, K. Mosina, Z. Sofer, B. Urbaszek. npj 2D Mater. Appl. **9**, 22 (2025).
[14] D.L. Gusenkov, R.A. Valeev, V.P. Piskorsky, A.I. Chernov, R.B. Morgunov. FTT **67**, *2*, 295 (2025) (in Russian).
[15] D.L. Gusenkov, A.I. Tiurin, M.V. Bakhmetiev, E.I. Kunitsyna, E.O. Chiglintsev, M.K. Tatmyshevskiy, A.I. Chernov, R.B. Morgunov. J. Phys. Chem. Solids **199**, 112589 (2025).
[16] E.J. Telford, D.G. Chica, M.E. Ziebel, K. Xie, N.S. Manganaro, C. Huang, J. Cox, A.H. Dismukes, X. Zhu, J.P.S. Walsh, T. Cao, C.R. Dean, X. Roy. Adv. Phys. Res. **2**, 2300036 (2023).
[17] L. Xie, J. Wang, J. Li, C. Li, Y. Zhang, B. Zhu, Y. Guo, Z. Wang, K. Zhang. Adv. Electron. Mater. **7**, 2000962 (2020).
[18] S.-H. Shim, T.S. Duffy, R. Jeanloz, C.-S. Yoo, V. Iota. Phys. Rev. B **69**, 144107 (2004).

Translated by T.Zorina